Cite this: *Phys. Chem. Chem. Phys.*, 2011, **13**, 2744–2747

www.rsc.org/pccp

PAPER

Photoionization-induced large-amplitude pendular motion in phenol$^+$–Kr

Mitsuhiko Miyazaki,[a] Akihiro Takeda,[a] Shun-ichi Ishiuchi,[a] Makoto Sakai,[a] Otto Dopfer*[b] and Masaaki Fujii*[a]

Received 28th September 2010, Accepted 10th November 2010
DOI: 10.1039/c0cp01961e

The dynamics of the intermolecular motion of the phenol$^+$–Kr cation generated by photoionization of the neutral π-structure is probed by picosecond time-resolved infrared spectroscopy. The spectrum at zero delay displays only the free OH stretch band of the π-structure. The appearance of the hydrogen-bonded OH stretch band of the H-structure after a few ps is due to ionization-induced π → H site switching. Spectra at long delay (> 20 ns) show that the Kr atom delocalizes from one π-site of the aromatic ring to the opposite π-site *via* the OH-site, like a pendular motion in the classical picture.

1. Introduction

Non-covalent interactions determine the structure, dynamics, and function of complex molecular systems, including biomolecular recognition, self assembly of supramolecules, and nanostructures.[1–3] These intermolecular forces are often classified as electrostatic and dispersion interactions. In this simple scheme, hydrogen bonds (H-bonds) are based on electrostatic interactions, whereas van der Waals forces (π-stacking) arise from dispersion. This subtle and complex competition between H-bonds and π-stacking may be viewed as competition between hydrophilic and hydrophobic binding motifs. Spectroscopic studies of isolated clusters in molecular beams provide the most direct experimental access to the salient properties of the intermolecular potential energy surface, such as geometries, binding energies, and the nuclear dynamics occurring on the surface.[2,4–9] Clusters of phenol with rare gas atoms (*e.g.*, Rg = Ar, Kr) are the simplest model systems to study the hydrophobic–hydrophilic competition, as they exhibit both dispersion forces *via* π-bonding to the aromatic ring and H-bonding to the acidic OH group.[10,11] For phenol–Rg clusters, this competition has been studied spectroscopically and theoretically in the neutral and cation ground electronic states (S_0, D_0).[7,10–22] In S_0, only the π-structure is observed,[7,20,21] because dispersion dominates the attraction. In D_0, the H-structure is more stable, as the additional electrostatic forces arising from the excess charge override dispersion (Fig. 1).[11–15,17,18,22] Hence, the Rg atom binds preferentially to the hydrophobic site in the neutral and to the hydrophilic site in the cation cluster. This change in the preferred recognition motif implies that ionization triggers an isomerization reaction, namely π → H site switching. The dynamics of this reaction has previously been monitored in real time for the phenol$^+$–Ar_2 trimer by time-resolved UV-UV-IR spectroscopy, yielding a time constant of 7.2 ps for the one-way, single-step elementary π → H switching reaction.[17,18] Significantly, the dynamical processes triggered by ionization of

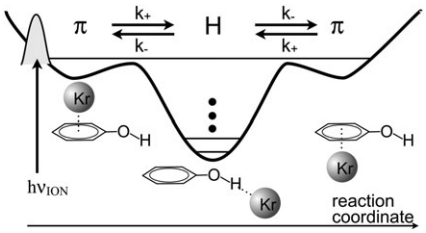

Fig. 1 Potential energy diagram of phenol$^+$–Kr along the reaction coordinate for the ionization-induced site switching reaction. The H-bound structure is the global minimum of the potential curve, whereas the two π-bound structures, in which Kr is attached to opposite sides of the aromatic ring, are local minima. Photoionization from the S_1 state of the π-bound phenol–Kr (using ν_{ION}) generates the π-bound cation due to vertical transitions according to the Franck–Condon principle. The rate constants for the forward and backward reactions used in the simple model are indicated.

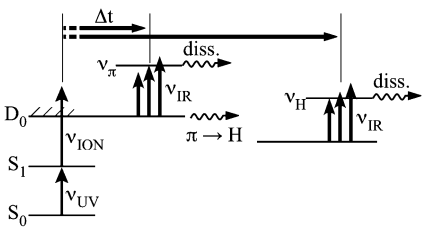

Fig. 2 Principle of picosecond time-resolved UV-UV-IR ion dip spectroscopy of phenol–Kr.

[a] *Chemical Resources Laboratory, Tokyo Institute of Technology, Yokohama 226-8503, Japan. E-mail: mfujii@res.titech.ac.jp*
[b] *Institut für Optik und Atomare Physik, Technische Universität Berlin, 10623 Berlin, Germany. E-mail: dopfer@physik.tu-berlin.de*

the simpler phenol$^+$–Kr dimer is qualitatively rather different, leading to the first real-time observation of a pendular motion in an isolated molecular cluster in the present work.

2. Experiment

The principle and setup for the measurement of the ps time-resolved UV-UV-IR ion dip spectra are described elsewhere (Fig. 2).[17,18] Briefly, phenol–Kr clusters are produced in a supersonic jet by expanding phenol seeded in a Ne/Kr mixture (9/1) at 1 bar through a pulsed valve into a vacuum chamber. Neutral phenol–Kr dimers are resonantly ionized *via* the first excited singlet state (S_1) using ps UV lasers. The first UV laser, ν_{UV}, excites phenol–Kr from the S_0 state to the S_1 origin at 36 295 cm^{-1} and the second UV laser, ν_{ION}, ionizes the excited cluster with little excess energy (<60 cm^{-1}) in the cation D_0 ground state.[13] The ions generated are extracted into a quadrupole mass spectrometer. While monitoring the mass-selected phenol$^+$–Kr ion current, a tunable ps IR laser, ν_{IR}, is fired and scanned in the OH stretching range with an adjustable delay (Δt) with respect to the ionizing UV lasers, ν_{UV} and ν_{ION}. The ion signal is amplified, integrated, and monitored as a function of ν_{IR} and/or Δt. If ν_{IR} is resonant with a vibrational transition of phenol$^+$–Kr, the cluster dissociates upon vibrational excitation, leading to a depletion (dip) in the phenol$^+$–Kr ion current. Thus, the IR spectrum of phenol$^+$–Kr is obtained by monitoring the depletion of the ion current as a function of ν_{IR}. The generation of the ps UV and IR laser radiation is described elsewhere.[17,18] The key parameters are 10 Hz repetition rate, ~3 ps pulse widths, ~20 cm^{-1} spectral widths, and pulse energies of 1, 5, and 70 μJ for ν_{UV}, ν_{ION}, and ν_{IR}, respectively. The two UV lasers and the IR laser beams are combined coaxially and focused by a CaF_2 lens with 250 mm focal length into the supersonic jet.

3. Results

Fig. 3 compares the ps time-resolved IR ion dip spectra of phenol$^+$–Kr obtained for delay times between −7 and +48 ps

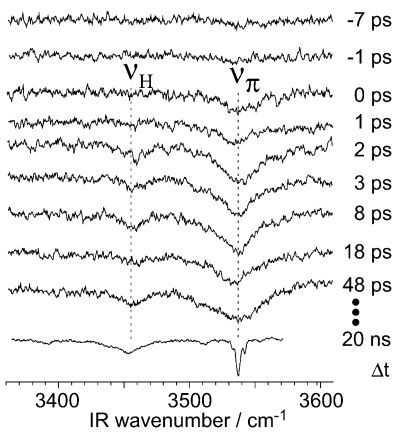

Fig. 3 Picosecond time-resolved IR ion dip spectra of phenol$^+$–Kr recorded in the OH stretching range for various delays Δt between the ionizing and IR lasers, ranging from −7 to +48 ps. For comparison, the IR dip spectrum measured for a delay of 20 ns by ns laser systems is also shown (ref. 13). The ν_H and ν_π frequencies of the H-bound and π-bound structures at 3452 and 3537 cm^{-1} are indicated by dotted lines.

with the IR spectrum at Δt = 20 ns delay recorded previously using ns lasers.[13] The IR spectrum at Δt = 10 ps is already similar in appearance to the one at Δt = 20 ns. The latter one displays a better spectral resolution due to the longer pulse duration of the ns lasers. Both IR spectra display ν_{OH} bands of the π-bound structure at 3537 cm^{-1} (ν_π) and the internally excited H-bound structure at 3452 cm^{-1} (ν_H) respectively. When the delay time is shortened toward the ionization event at zero delay, the ν_H band decreases in its intensity and disappears at Δt = 2 ps. This observation directly proves that only the π-bound structure is generated by photoionization and that the Kr atom switches the binding site from above the benzene ring to the OH group after the ionization event.

This phenomenon, described as ionization-induced π→H site switching, is similar to that observed previously for phenol$^+$–Ar_2,[17,18] in which one of the π-bound Ar atoms isomerizes to the OH binding site upon ionization. The qualitative difference between both systems is the yield of the ionization-induced switching reaction. In phenol$^+$–Ar_2, the ν_π band appears upon photoionization at zero delay and essentially disappears at Δt = 10 ps, implying a 100% yield for the π → H reaction. Thus, for this system, the ionization-induced π → H switch is an elementary reaction with a measured lifetime of 7.2 ps. In contrast, for phenol$^+$–Kr, the ν_π band remains with high intensity even for delay times as long as 20 ns after photoionization, indicating that there are qualitative differences in the reaction mechanisms for both systems.

To shed further light on the switching mechanism in phenol$^+$–Kr, the time evolutions of the ν_π and ν_H resonances are compared in Fig. 4. These time profiles are obtained by fixing ν_{IR} to the ν_π and ν_H bands and scanning the delay time Δt. The ν_π signal rises immediately after the ionization event at zero delay and then gradually decays but significant intensity remains even after 100 ps. In contrast, the ν_H signal rises slowly from zero at Δt = 0 and reaches an almost constant value after ~20 ps. The peak near Δt = 0 marked by an asterisk is due to a coherent spike and not the formation of the H-bound cluster. The spike represents the cross correlation function between ν_{ION} and ν_{IR} and demonstrates that the overall time resolution of the experimental approach is ~3 ps. The immediate rise of the ν_π band and the slow increase of the ν_H band are consistent with the time-resolved IR spectra shown in Fig. 3. Moreover, the rise of the ν_π signal is almost the same as the cross correlation between ν_{ION} and ν_{IR}.

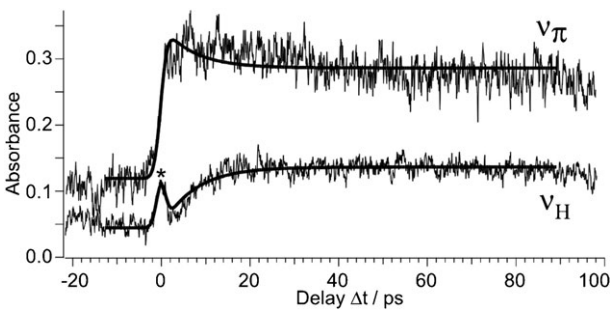

Fig. 4 Time evolutions of the ν_H and ν_π bands at 3452 and 3537 cm^{-1} (Fig. 3). The peak at around 0 ps marked by an asterisk is due to a coherent spike. Also shown are the fitted time evolutions derived from the rate equation model.

The corresponding curves for phenol$^+$–Ar_2 show a more simple time evolution.[18] They arise from a one-way, single-step elementary $\pi \rightarrow H$ switching reaction with a single-exponential rise and decay with a lifetime of $\tau = 7.2$ ps (corresponding to a rate constant of $k = \tau^{-1} = 0.14$ ps^{-1}), *i.e.*, the ν_π signal decays completely to zero, while with the same time constant the ν_H signal rises from zero to full amplitude. If phenol$^+$–Kr were to have the same reaction mechanism, the ν_π signal should completely disappear with the same time constant as the ν_H signal appears, in clear disagreement with the experiment (Fig. 4). One may speculate that the long-lived signal of the ν_π band may be produced by another nonreactive species formed by the same ionization event. However, this possibility can be ruled out by the previous experiment using nanosecond lasers.[13] In these experiments, the appearance of both ν_π and ν_H at long delay was the same even when the cluster cation was prepared selectively in the vibrational ground state with 7 cm^{-1} excess energy for ionization.[13,19] Thus, the long survival of the ν_π signal suggests that the reaction mechanism in phenol$^+$–Kr is more complex than in phenol$^+$–Ar_2. In fact, the time evolution of the phenol$^+$–Kr signals can readily be rationalized by taking into account the $H \rightarrow \pi$ back reaction, which leads to a constant nonvanishing equilibrium population of the π-bound and H-bound configurations for long delay times.

4. Discussion

To analyze the dynamical processes in more detail, the time evolutions of the ν_π and ν_H signals are simulated according to the following rate equations (Fig. 1):

$$\frac{d}{dt}[\pi] = -k_+[\pi] + 2k_-[H] \quad (1)$$

$$\frac{d}{dt}[H] = k_+[\pi] - 2k_-[H] \quad (2)$$

Here, [H] and [π] represent the populations in the H- and the two π-structures, respectively. Assuming $[\pi(t = 0)] = 1$ and $[H(t = 0)] = 0$, eqn (1) and (2) are solved as follows:

$$[\pi] = \frac{1}{k_+ + 2k_-}[2k_- + k_+ \exp\{-(k_+ + 2k_-)t\}] \quad (3)$$

$$[H] = \frac{k_+}{k_+ + 2k_-}[1 - \exp\{-(k_+ + 2k_-)t\}] \quad (4)$$

$$\lim_{t\rightarrow\infty}\frac{[\pi]}{[H]} = \frac{2k_-}{k_+} \quad (5)$$

Fitting of the time evolution of the ν_H band yields $k_+ + 2k_- = 0.135$ ps^{-1}. From the calculated ratio of ~4 for the transition cross sections of ν_π and ν_H,[13] the ratio $2k_-/k_+ = 1.63$ is estimated from the spectrum at 20 ns, which is assumed to be one at equilibrium. Finally, values of k_+ and k_- are obtained as 0.051 and 0.042 ps^{-1}, corresponding to $\tau_+ = 20$ ps and $\tau_- = 24$ ps, respectively. The $\pi \rightarrow H$ forward reaction rate k_+ is thus three times slower than the corresponding rate observed for the phenol$^+$–Ar_2 trimer ($k = 0.14$ ps^{-1}). This difference is consistent with the mass ratio of the two rare gas atoms ($M_{Kr}/M_{Ar} \approx 2$). As can be seen in Fig. 4, the best fit reproduces the experimental time evolutions of both the ν_π and ν_H bands rather well. Although the quantitative reproduction is not perfect using this simple model, the occurrence of the $H \rightarrow \pi$ back reaction is evident from the observation of the ν_π band at long delay times, which is the principal difference between phenol$^+$–Kr and phenol$^+$–Ar_2.

The different behavior of the $\pi \rightarrow H$ switching dynamics in phenol$^+$–Kr and phenol$^+$–Ar_2 is attributed to the lack of the $H \rightarrow \pi$ back reaction in the latter system due to efficient intracluster vibrational energy redistribution (IVR) occurring after the site switching. In phenol$^+$–Kr, IVR is much less efficient because of the lower density of states. Phenol$^+$–Kr has three low-frequency intermolecular modes (two bending and one stretching vibration) and the reaction coordinate for $\pi \rightarrow H$ site switching is a linear combination of all three modes. Thus, the nascent H-bound conformation generated by $\pi \rightarrow H$ site switching is populating highly excited levels involving all three intermolecular modes. According to *ab initio* calculations at the MP2/aug-cc-pVTZ level, the H-structure is about 400 cm^{-1} more stable than the π-structure. In the present experiment, the π-bound cation is prepared with small vibrational excess energy (<60 cm^{-1}). Thus, the calculated energy difference between the π- and H-structures of 400 cm^{-1} is close to the vibrational excess energy after the $\pi \rightarrow H$ switch. At this excess energy, the density of available bath modes for IVR is rather low. First, there are only few intramolecular modes of phenol$^+$ with frequencies lower than 500 cm^{-1}, namely $\nu_{11} = 177$, $\nu_{16a} = 348$, $\nu_{18b} = 411$, and $\nu_{16b} = 428$ cm^{-1}.[23] Second, as all three intermolecular modes of phenol$^+$–Kr are involved in the reaction coordinate, they cannot act as bath modes. The low density of bath states results in small IVR rates, which enables the efficient $H \rightarrow \pi$ back reaction in phenol$^+$–Kr. As a consequence, the populations of π-bound and H-bound structures quickly approach equilibrium after ionization.

The energy difference for H- and π-bonding in phenol$^+$–Ar_2[12,15,22] is slightly smaller than for phenol$^+$–Kr, leading to somewhat less vibrational excess energy after the $\pi \rightarrow H$ switch. Thus, similar to phenol$^+$–Kr, the intramolecular phenol$^+$ modes will not strongly contribute to the density of states. However, the available intermolecular mode density is drastically larger for phenol$^+$–Ar_2. In a zero-order local mode picture, the six intermolecular modes are divided into three of the isomerizing Ar ligand and three of the remaining π-bound Ar spectator ligand. The latter ones can act as efficient bath modes, leading to rapid IVR in the nascent hot H-bound configuration, which quickly transfers vibrational excess energy from the reaction coordinate into the intermolecular degrees of freedom of the spectator ligand. As a result, the $H \rightarrow \pi$ back reaction is efficiently quenched for phenol$^+$–Ar_2.[24] In a classical view, the hot H-bound Ar ligand is cooling down by heating the spectator Ar ligand.

There are two equivalent π-bound sites in phenol$^+$–Kr, which are equally populated by the $H \rightarrow \pi$ back reaction from the hot H-bound cluster (Fig. 1). In the classical description, ionization of phenol–Kr triggers the large-amplitude pendular motion between phenol$^+$ and Kr, whereby the Kr atom moves from one π-site to the other π-site opposite of the aromatic ring *via* the OH site.

Quantum mechanically, photoionization of π-bound neutral phenol–Kr generates a wavepacket on the cation potential, which is initially localized at the π-bound region due to the vertical transition given by the Franck–Condon principle (Fig. 1). Subsequently, the wavepacket quickly propagates toward the center of the potential and spreads out in the whole region between the two potential walls by further dephasing, covering both π-bound structures and the H-bound structure. This limit corresponds to the near-equilibrium situation observed spectroscopically after a delay of ~20 ps.

In summary, ps time-resolved IR spectroscopy has been used to monitor a large-amplitude pendular motion in the phenol$^+$–Kr cluster triggered by resonant photoionization of the π-bound neutral precursor. The spectroscopic results provide evidence that the Kr atom delocalizes from one π-site to the other π-site opposite of the aromatic benzene ring *via* the OH site, just like a pendular motion in the classical picture. This is the first direct observation for such an ionization-induced intermolecular dynamical process in a molecular cluster. As the ionization-induced π → H switch in the preferred recognition motif between acidic aromatic molecules and nonpolar ligands has been recognized recently as a general phenomenon,[11] the dynamics observed here for phenol$^+$–Kr will be a general property of molecular recognition phenomena involving ionization processes of such fundamental (bio)molecular building blocks interacting with a hydrophobic nonpolar environment. There is preliminary evidence that the phenol$^+$–Ar dimer shows the same phenomenon, and efforts in characterizing the dynamics in this system by time-resolved IR spectroscopy are in progress.

Acknowledgements

This work was supported by a Grant-in-Aid for Scientific Research KAKENHI in the priority area 477 from MEXT (Japan) and the Core-to-Core Program from Japan Society for Promotion of Science and the Deutsche Forschungsgemeinschaft (DO 729/4).

References

1 P. Hobza and K. Müller-Dethlefs, *Non-covalent interactions*, The Royal Society of Chemistry, Cambridge, 2010.
2 Brutschy and G. E. P. Hobza, *Chem. Rev.*, 2000, **100**, 3861–4264.
3 E. A. Meyer, R. K. Castellano and F. Diederich, *Angew. Chem., Int. Ed.*, 2003, **42**, 1210–1250.
4 M. Miyazaki, A. Fujii, T. Ebata and N. Mikami, *Science*, 2004, **304**, 1134–1137.
5 R. N. Pribble and T. S. Zwier, *Science*, 1994, **265**, 75–79.
6 J.-W. Shin, N. I. Hammer, E. G. Diken, M. A. Johnson, R. S. Walters, T. D. Jaeger, M. A. Duncan, R. A. Christie and K. D. Jordan, *Science*, 2004, **304**, 1137–1140.
7 I. Kalkman, C. Brand, T. C. Vu, W. L. Meerts, Y. N. Svartsov, O. Dopfer, K. Müller-Dethlefs, S. Grimme and M. Schmitt, *J. Chem. Phys.*, 2009, **130**, 224303.
8 A. Stolow, A. E. Bragg and D. M. Neumark, *Chem. Rev.*, 2004, **104**, 1719–1757.
9 T. Ebata, A. Fujii and N. Mikami, *Int. Rev. Phys. Chem.*, 1998, **17**, 331–361.
10 C. E. H. Dessent and K. Müller-Dethlefs, *Chem. Rev.*, 2000, **100**, 3999–4022.
11 O. Dopfer, *Z. Phys. Chem.*, 2005, **219**, 125–168.
12 N. Solcà and O. Dopfer, *J. Phys. Chem. A*, 2001, **105**, 5637–5645.
13 A. Takeda, H. S. Andrei, M. Miyazaki, S. Ishiuchi, M. Sakai, M. Fujii and O. Dopfer, *Chem. Phys. Lett.*, 2007, **443**, 227–231.
14 N. Solcà and O. Dopfer, *Chem. Phys. Lett.*, 2000, **325**, 354–359.
15 N. Solcà and O. Dopfer, *J. Mol. Struct.*, 2001, **563/564**, 241–244.
16 A. Fujii, T. Sawamura, S. Tanabe, T. Ebata and N. Mikami, *Chem. Phys. Lett.*, 1994, **225**, 104–107.
17 S. Ishiuchi, M. Sakai, Y. Tsuchida, A. Takeda, Y. Kawashima, M. Fujii, O. Dopfer and K. Müller-Dethlefs, *Angew. Chem., Int. Ed.*, 2005, **44**, 6149–6151.
18 S. Ishiuchi, M. Sakai, Y. Tsuchida, A. Takeda, Y. Kawashima, O. Dopfer, K. Müller-Dethlefs and M. Fujii, *J. Chem. Phys.*, 2007, **127**, 114307.
19 S. Ullrich, G. Tarczay and K. Müller-Dethlefs, *J. Phys. Chem. A*, 2002, **106**, 1496–1503.
20 S. Ishiuchi, Y. Tsuchida, O. Dopfer, K. Müller-Dethlefs and M. Fujii, *J. Phys. Chem. A*, 2007, **111**, 7569–7575.
21 J. Makarewicz, *J. Chem. Phys.*, 2006, **124**, 084310.
22 J. Černý, X. Tong, P. Hobza and K. Müller-Dethlefs, *Phys. Chem. Chem. Phys.*, 2008, **10**, 2780–2784.
23 O. Dopfer, G. Reiser, K. Müller-Dethlefs, E. W. Schlag and S. D. Colson, *J. Chem. Phys.*, 1994, **101**, 974.
24 C. Walter, R. Kritzer, A. Schubert, C. Meier, O. Dopfer and V. Engel, *J. Phys. Chem. A*, 2010, **114**, 9743–9748.